Journal of Solid State Chemistry **164,** 332–338 (2002)
doi:10.1006/jssc.2001.9480, available online at http://www/idealibrary.com on IDEAL®

Chemical Synthesis and Properties of Spinel $Li_{1-x}Co_2O_{4-\delta}$

S. Choi and A. Manthiram[1]

Materials Science and Engineering Program, ETC 9.104, The University of Texas at Austin, Austin, Texas 78712

Received August 29, 2001; in revised form November 13, 2001; published online February 12, 2002

Spinel $Li_{1-x}Co_2O_{4-\delta}$ samples with $0.44 \le (1-x) \le 1$ have been synthesized by chemically extracting lithium with the oxidizer NO_2BF_4 in acetonitrile medium from the LT-$LiCoO_2$ synthesized at 400°C. Rietveld analysis of the X-ray diffraction data reveals that the $Li_{1-x}Co_2O_{4-\delta}$ samples adopt the normal cubic spinel structure with a cation distribution of $(Li_{1-x})_{8d}[Co_2]_{16d}O_{4-\delta}$. Redox iodometric titration data indicate that the LT-$LiCoO_2$ tends to lose oxygen on extracting lithium and the spinel $Li_{1-x}Co_2O_{4-\delta}$ samples are oxygen-deficient. Both infrared spectroscopic and magnetic susceptibility data suggest that the $LiCo_2O_{4-\delta}$ spinel is metallic with itinerant electrons. The tendency to lose oxygen on extracting lithium from the LT-$LiCoO_2$ and the observed metallic behavior of the spinel $LiCo_2O_{4-\delta}$ are explained on the basis of a qualitative band diagram. © 2002 Elsevier Science (USA)

1. INTRODUCTION

Transition metal oxides consisting of highly oxidized redox couples such as $Mn^{3+/4+}$, $Fe^{3+/4+}$, $Co^{3+/4+}$, $Ni^{3+/4+}$, and $Cu^{2+/3+}$ have a near-equivalence of the metal:d and oxygen: 2*p* energies and are characterized by a small charge transfer gap (1). Such oxides have drawn considerable attention in recent years both from scientific and technological points of view due to their interesting electronic properties such as high-temperature superconductivity, colossal magnetoresistance, and metal–insulator transitions (2–6). However, most of the previous studies have focused primarily on oxides having the AMO_3 perovskite structure or perovskite-related intergrowth structures such as the Ruddlesden–Popper series $A_{n+1}M_nO_{3n+1}$ ($n=1$, 2, and 3) in which the transition metal M^{n+} ions are bonded to the oxide ions with 180° *M*–O–*M* bonds. Relatively, less information is available on oxides having 90° *M*–O–*M* and direct *M*–*M* bonds in which the transition metal ions exist in a high oxidation state. Some examples of such systems are oxides having the *M*O rock salt or AM_2O_4 spinel structures. The lack of a detailed investigation of their electronic properties is mainly due to the difficulties in accessing these oxides having unusually high oxidation states such as Fe^{4+}, Co^{4+}, and Ni^{4+}.

Such oxides with high oxidation states and 90° *M*–O–*M* bonds are, however, known to be formed during the electrochemical charging process of the Li*M*O_2 (*M* = Co and Ni) cathodes in lithium ion cells (7–12); the $LiMO_2$ oxides have an ordered rock salt structure isotypic with α-$NaFeO_2$ in which the Li^+ and M^{3+} ions occupy the alternate (111) planes of the rock salt structure. Unfortunately, it is difficult to chemically characterize and evaluate the electrical and magnetic properties of the products obtained by electrochemical charging as they will be contaminated by carbon, binder, and electrolyte. Recently, we showed that bulk samples of $Li_{1-y}Co_{1-\eta}Ni_\eta O_{2-\delta}$ ($0 \le y \le 1$ and $0 \le \eta \le 1$) with a 90° metal–oxygen–metal and direct metal–metal bonding can be accessed by chemically extracting lithium from Li*M*O_2 (*M* = Co and Ni) at ambient temperature with an oxidizing agent, NO_2PF_6, in acetonitrile medium (13, 14). While the $Li_{1-y}CoO_{2-\delta}$ samples were found to show a semiconductor-to-metal transition for $(1-y) < 0.77$ due to a partially filled t_{2g} band associated with the low-spin $Co^{3+/4+}$ ion, the $Li_{1-y}NiO_{2-\delta}$ samples were found to be semiconducting for the entire value of $0 \le y \le 1$ due to a completely filled t_{2g} band associated with the $Ni^{3+/4+}$ ion.

We present in this paper the synthesis of spinel $Li_{1-x}Co_2O_{4-\delta}$ by chemically extracting lithium from the low-temperature form of $LiCoO_2$ synthesized at 400°C using the oxidizer NO_2BF_4 in acetonitrile medium. We also present the characterization of the $Li_{1-x}Co_2O_{4-\delta}$ samples by wet-chemical analysis to determine the lithium and oxygen contents, infrared spectroscopy to determine the electrical conduction behavior, and magnetic property measurements. The properties of the spinel $Li_{1-x}Co_2O_{4-\delta}$ are compared with those of the layered $Li_{1-y}CoO_{2-\delta}$, both having 90° Co–O–Co and direct Co–Co interactions.

$LiCoO_2$ synthesized at low temperatures ($T \approx 400$°C) is known to adopt a structure that is different from that synthesized at 900°C and it has been designated as LT-$LiCoO_2$ (15–21). LT-$LiCoO_2$ has been shown from X-ray

[1]To whom correspondence should be addressed.

0022-4596/02 $35.00

diffraction and single-crystal electron diffraction studies to consist of a major lithiated spinel-like phase with a cation distribution of $\{Li_2\}_{16c}[Co_2]_{16d}$ O_4 and a minor layered $LiCoO_2$ phase (15–18). The LT-$LiCoO_2$ was known previously to give the $LiCo_2O_4$ spinel phase on extracting 50% of lithium with aqueous acids. We present here the extraction of various amounts of lithium from LT-$LiCoO_2$ with an oxidizing agent in a nonaqueous medium and the characterization of the products $Li_{1-x}Co_2O_{4-\delta}$ $(0.44 \le (1-x) \le 1)$.

2. EXPERIMENTAL

LT-$LiCoO_2$ was prepared by firing a stoichiometric mixture of Li_2CO_3 and Co_3O_4 at 400°C in air for 1 week. Chemical extraction of lithium from the LT-$LiCoO_2$ was carried out by stirring approximately 300 mg of the powdered sample for 2 days under an argon atmosphere in an acetonitrile medium containing various amounts of the oxidizing agent NO_2BF_4. The lithium extraction reaction can be represented as

$$LiCoO_2 + yNO_2BF_4 \rightarrow Li_{1-y}CoO_2 + yNO_2 + yLiBF_4. \quad [1]$$

The product formed after the reaction was washed with acetonitrile several times under an argon atmosphere using a schlenk line to remove the by-product $LiBF_4$ and dried under vacuum. The dried samples were then stored in a vacuum desiccator.

The lithium contents in the sample before and after the chemical delithiation process were determined by atomic adsorption spectroscopy. Structural characterization of the samples was carried out with X-ray powder diffraction. Lattice parameters and cation distributions were refined by the Rietveld method using the DBWS-9411 PC program (22). The oxidation state of cobalt and the oxygen content were determined by iodometric titration employing KI and sodium thiosulfate solutions (23).

Thermogravimetric analysis (TGA) data were carried out with a Perkin-Elmer series 7 thermal analyzer. Infrared spectra were recorded with a Perkin-Elmer AVATAR 360 FT-IR spectrometer using KBr pellets. Magnetic measurements were carried out with a Quantum design SQUID magnetometer in the temperature range of $5 < T < 320$ K under zero-field-cooled and field-cooled conditions.

3. RESULTS AND DISCUSSION

3.1. Structural and Compositional Characterizations

Table 1 gives the chemical analysis data of LT-$LiCoO_2$ and the LT-$Li_{1-y}CoO_{2-\delta}$ (or $Li_{1-x}Co_2O_{4-\delta}$ in the spinel notation) samples obtained by chemically extracting lithium from LT-$LiCoO_2$. The data show that the end member has a lithium content of 0.44 in $Li_{1-x}Co_2O_{4-\delta}$, indicating that only 78% of the lithium could be chemically extracted from LT-$LiCoO_2$. Removal of lithium beyond $(1-x) = 0.44$ was not possible even with a large excess of the oxidizer NO_2BF_4 or by treating $Li_{0.44}Co_2O_{4-\delta}$ with an excess fresh solution of NO_2BF_4. This is in contrast to the results found with the HT-$LiCoO_2$ that was prepared at 900°C and has the rhombohedral layer structure of α-$NaFeO_2$. All the lithium could be completely extracted from the layered HT-$LiCoO_2$ to give $CoO_{2-\delta}$ with a HT-$LiCoO_2$:NO_2BF_4 molar ratio of 1:1.5 in the reaction mixture (13,14). The difficulty in removing all the lithium from the LT-$LiCoO_2$, attests to the fact that it is structurally different from the conventionally prepared HT-$LiCoO_2$, as has been found before (15–21). The removal of lithium from the 8*a* tetrahedral sites of the spinel lattice $(Li_{1-x})_{8a}[Co_2]O_{4-\delta}$ obtained from LT-$LiCoO_2$ (see below) requires higher energy than that from the 16*c* octahedral sites of the spinel structure or 3*a* sites of the layer structure. This is consistent with the higher voltage generally observed for the removal of tetrahedral site lithium ions compared to the octahedral site lithium ions of the spinel lattice (24).

TABLE 1
Wet-Chemical Analysis Data of LT-$LiCoO_2$ and $Li_{1-x}Co_2O_{4-\delta}$ Samples

Molar ratio of LT-$LiCoO_2$:NO_2BF_4	Sample composition	Oxidation state of cobalt	Spinel notation
	LT-$LiCoO_2$	3.03+	$\{Li_2\}_{16c}[Co_2]_{16d}O_{4.03}$
1:0.8	$Li_{0.5}CoO_{1.94}$	3.37+	$(Li)_{8a}[Co_2]_{16d}O_{3.87}$
1:2.2	$Li_{0.3}CoO_{1.74}$	3.18+	$(Li_{0.6})_{8a}[Co_2]_{16d}O_{3.48}$
1:3.1	$Li_{0.22}CoO_{1.68}$	3.14+	$(Li_{0.44})_{8a}[Co_2]_{16d}O_{3.36}$

Figure 1 shows the X-ray diffraction patterns of all the samples listed in Table 1. The X-ray diffraction pattern of the parent LT-$LiCoO_2$ (Fig. 1a) could be indexed on the basis of the cubic lithiated spinel structure, which is in agreement with the previous literature data (15–18). The X-ray patterns of the lithium-extracted samples $Li_{1-x}Co_2O_{4-\delta}$ $(0.44 \le (1-x) \le 1)$ could also be indexed on the basis of the spinel structure with the space group $Fd\bar{3}m$ (Figs. 1b–1d). Figure 2 shows the Rietveld refinement data of the $Li_{1-x}Co_2O_{4-\delta}$ $(0.44 \le (1-x) \le 1)$ samples. The refinements were carried out with fixed values for site occupancy. A good agreement between the observed and calculated X-ray patterns with low *R* factors reveals that these samples adopt the normal spinel structure with the cation distributions indicated in Fig. 2 and Table 1. The lattice parameter of the $Li_{1-x}Co_2O_{4-\delta}$ samples decreases on going from the $(1-x) = 1$ sample (Fig. 2a) to the $(1-x) = 0.6$ sample (Fig. 2b) and then increases on going to the $(1-x) = 0.44$ sample (Fig. 2c), but the changes are extremely small. Although one would anticipate a smooth

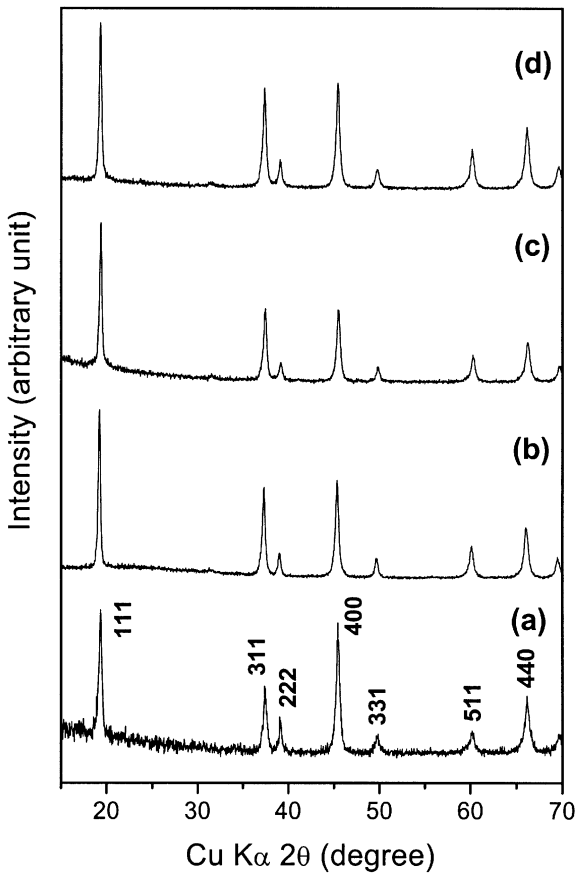

FIG. 1. X-ray diffraction patterns of LT-$LiCoO_2$ and the $Li_{1-x}Co_2O_{4-\delta}$ spinel oxides obtained from it by chemical lithium extraction: (a) LT-$LiCoO_2$, (b) $LiCo_2O_{3.87}$, (c) $Li_{0.6}Co_2O_{3.48}$, and (d) $Li_{0.44}Co_2O_{3.36}$.

decrease in lattice parameter with decreasing lithium content due to the expected increase in the oxidation state of cobalt, the system tends to lose oxygen from the lattice as discussed in the next paragraph, which leads to a decrease in the oxidation state of cobalt on extracting lithium. While the decrease in the oxidation state will cause an increase in lattice parameter, the increase in the concentration of oxygen vacancies may cause a decrease in lattice parameter. A balance between these two opposing effects appears to cause little or an insignificant change in the overall lattice parameter with lithium content.

Table 1 gives the oxidation state of cobalt and the oxygen content determined by iodometric titration for the various samples. While the initial LT-$LiCoO_2$ has an oxygen content of around 2 (or 4 in the spinel notation), the delithiated samples have lower oxygen content values. The oxidation state of cobalt increases with initial lithium extraction from 3.03+ at LT-$LiCoO_2$ to 3.37+ at $(1-x)=1$ in $Li_{1-x}Co_2O_{4-\delta}$, but decreases thereafter to 3.14+ at $(1-x)=0.44$. The data reveal that the system loses oxygen from the lattice at deep lithium extraction. Although the formation of $LiCo_2O_4$ spinel has been reported before on extracting lithium from the LT-$LiCoO_2$ with dilute acids (18), this is the first time that these samples have been chemically characterized for oxygen contents. The chemical analysis data in Table 1 reveal that it will be difficult to access the oxygen stoichiometric spinel $LiCo_2O_4$ without oxygen vacancies.

The observation of the tendency to lose oxygen on extracting lithium from the LT-$LiCoO_2$ is consistent with the result found for the layered $Li_{1-y}CoO_{2-\delta}$ samples obtained by extracting lithium from the HT-$LiCoO_2$ (13,14). The latter system was also found to lose oxygen on deep lithium extraction with $(1-y)<0.6$ in $Li_{1-y}CoO_{2-\delta}$ (13). However, at a given lithium content $(1-x)$, the spinel $Li_{1-x}Co_2O_{4-\delta}$ samples obtained from the LT-$LiCoO_2$ appear to lose more oxygen than the layered $Li_{1-y}CoO_{2-\delta}$ samples obtained from the HT-$LiCoO_2$. For example, the end member with the layer structure has an oxidation state of 3.34+ for cobalt and an oxygen content of 1.67 while the end member $Li_{0.44}Co_2O_{4-\delta}$ has an oxidation state of 3.14+ for cobalt and an oxygen content of 3.36.

The loss of oxygen from the $Li_{1-x}Co_2O_{4-\delta}$ lattice at deep lithium extraction is due to an overlap of the $Co^{3+/4+}$:t_{2g}

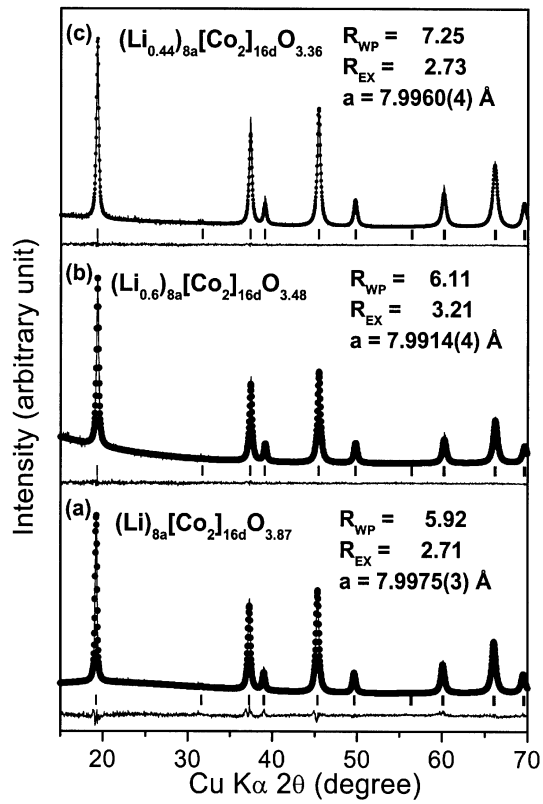

FIG. 2. Rietveld refinement results of $Li_{1-x}Co_2O_{4-\delta}$ spinel oxides: (a) $LiCo_2O_{3.87}$, (b) $Li_{0.6}Co_2O_{3.48}$, and (c) $Li_{0.44}Co_2O_{3.36}$. The observed and calculated X-ray profiles, peak positions, and the difference between the observed and calculated profiles are shown.

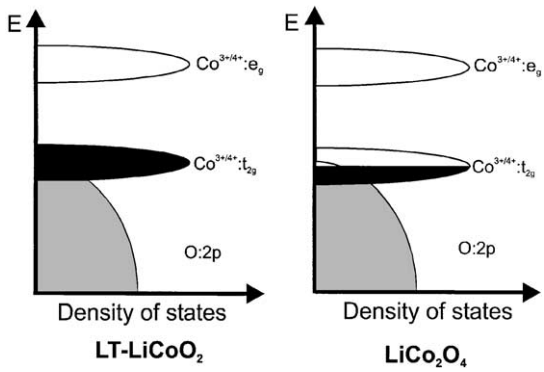

FIG. 3. Qualitative energy diagrams of LT-$LiCoO_2$ and $LiCo_2O_4$ spinel.

band with the top of the O:2*p* band as shown in Fig. 3. Such an overlap leads to the removal of electrons from both the $Co^{3+/4+}$:t_{2g} band and the O:2*p* band at deep lithium extraction. Removal of a significant amount of electrons from the O:2p band will result in an oxidation of the O^{2-} ions and an eventual evolution of oxygen from the lattice. This conclusion is consistent with the spectroscopic observation that the holes are introduced into the O:2*p* band rather than into the Co:3*d* band during charging of the HT-$LiCoO_2$ cathodes in lithium ion cells (25, 26). Additionally, the tendency of the spinel $Li_{1-x}Co_2O_{4-\delta}$ samples to lose more oxygen compared to the layered $Li_{1-y}CoO_{2-\delta}$ samples at a given lithium content reveals that the $Co^{3+/4+}$:t_{2g} energy lies slightly deep into the top of the O:2*p* band in the spinel compared to that in the layer structure. This conclusion is also consistent with the difficulty to extract all the lithium from the spinel $Li_{1-x}Co_2O_{4-\delta}$.

Figure 4 shows the TGA plot of the $LiCo_2O_{4-\delta}$ spinel recorded in air. The initial small weight loss below 200°C is due to the adsorbed moisture. This is confirmed by the fact that the as-prepared and the 200°C heated $Li_{1-x}Co_2O_{4-\delta}$ samples show nearly the same oxidation state for cobalt as revealed by the iodometric titration. The weight loss occurring above 200°C in Fig. 4 is due to the loss of oxygen from the lattice according to the disproportionation reaction given below:

$$LiCo_2O_{3.87} \rightarrow LiCoO_2 + 0.33Co_3O_4 + 0.27O_2\uparrow . \quad [2]$$

The formation of $LiCoO_2$ and Co_3O_4 was confirmed by an X-ray diffraction analysis of the products obtained by heating the $LiCo_2O_{3.87}$ sample to various temperatures (Fig. 5). Reflections corresponding to Co_3O_4 begin to appear at $T = 300$°C. The data reveal that the $Li_{1-x}Co_2O_{4-\delta}$ spinel is metastable and it disproportionates to thermodynamically more stable phases above 200°C.

3.2. Electrical Conduction

Since the $Li_{1-x}Co_2O_{4-\delta}$ samples were obtained by a soft chemistry synthesis procedure and are metastable, it is difficult to make sintered, dense pellets that would be needed for direct resistivity measurements. However, a qualitative idea about the conduction process can be obtained by examining the infrared spectra of the samples (13, 14, 27). Accordingly, the infrared spectra of the $Li_{1-x}Co_2O_{4-\delta}$ samples in the region corresponding to the bending and stretching modes of the CoO_6 octahedra are shown in Fig. 6 along with that of the parent LT-$LiCoO_2$.

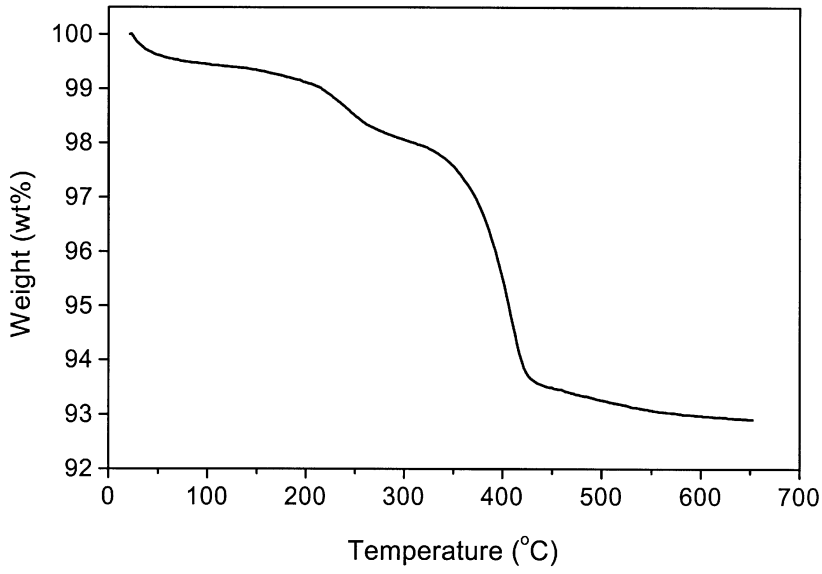

FIG. 4. TGA plot of $LiCo_2O_{4-\delta}$ spinel recorded in air at a heating rate of 2°C/min.

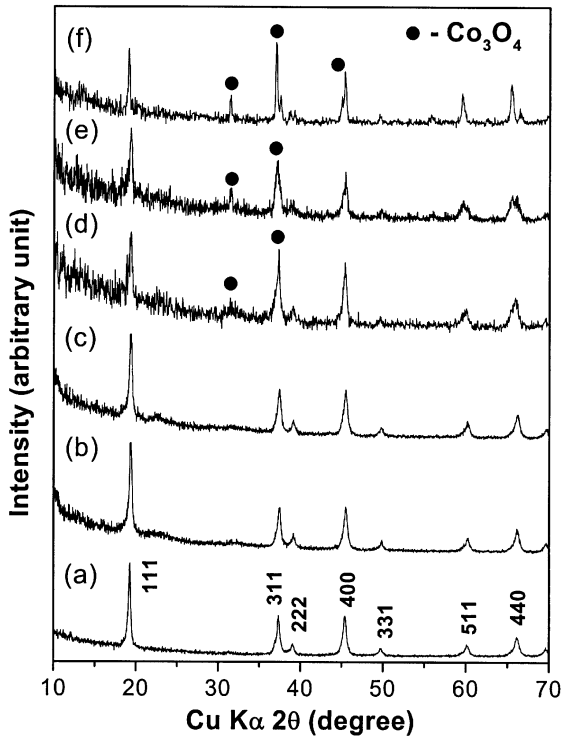

FIG. 5. X-ray diffraction patterns of (a) $LiCo_2O_{3.87}$ and after heating it at, (b) 150°C, (c) 200°C, (d) 300°C, (e) 400°C, and (f) 800°C.

The LT-$LiCoO_2$ sample (Fig. 6a) shows well-defined absorption bands indicating a semiconducting behavior similar to that found in the case of HT-$LiCoO_2$ (13,14,28). On the other hand, the $LiCo_2O_{3.87}$ sample (Fig. 6b) obtained by extracting 50% of lithium from the LT-$LiCoO_2$ shows no characteristic absorption bands indicating a metallic behavior. The observation of a semiconductor-to-metal transition on going from lithiated spinel LT-$LiCoO_2$ to the spinel $LiCo_2O_{3.87}$ is in accordance with the semiconductor-to-metal transition observed around $y = 0.77$ for the $Li_{1-y}CoO_{2-\delta}$ layered oxides obtained from the HT-$LiCoO_2$ (13). As the electrical conductivity increases, the optical skin depth of the incident beam decreases, which leads to a probing of only the surface of the sample and a resulting decrease in the intensity of the absorption bands. Alternatively, in the case of metallic systems with itinerant electrons, the free electrons are able to oscillate to any frequency of the incident radiation, resulting in no characteristic absorption. However, weak absorption bands begin to appear on extracting more lithium from $LiCo_2O_{4-\delta}$ to give the cation-deficient spinel phases $Li_{0.6}Co_2O_{4-\delta}$ (Fig. 6c) and $Li_{0.44}Co_2O_{4-\delta}$ (Fig. 6d). This is because the extraction of a large amount of lithium leads to a decrease in the oxidation state of cobalt and the formation of a significant amount of oxygen vacancies. The presence of a large amount of oxygen vacancies can perturb the periodic potential and introduce localized states at the band edge and thereby decrease the electrical conductivity.

The observations of semiconducting behavior for the LT-$LiCoO_2$ and metallic behavior for the spinel $LiCo_2O_{4-\delta}$ could be understood by considering the qualitative energy diagram given in Fig. 3. In the case of LT-$LiCoO_2$ with a low-spin Co^{3+}:$3d^6$ electronic configuration, a completely filled t_{2g} band leads to semiconducting behavior. In the case of $LiCo_2O_{4-\delta}$ spinel with a low spin $Co^{(3.5-\delta)+}$:$3d^{5.5+\delta}$ electronic configuration, a partially filled t_{2g} band leads to metallic conductivity due to the direct Co–Co interaction across the shared octahedral edge in the spinel structure. However, such an interaction will weaken with a decreasing oxidation state of cobalt and an increasing concentration of oxygen vacancies, resulting in a weak localized behavior for the $1-x = 0.6$ and 0.44 samples in $Li_{1-x}Co_2O_{4-\delta}$.

3.3. Magnetic Properties

Figure 7 shows the variations of the magnetic susceptibility of LT-$LiCoO_2$ and spinel $Li_{1-x}Co_2O_{4-\delta}$ with temperature. Although the curves shown in Fig. 7 refer to field-cooled data, no significant difference was observed between the zero-field-cooled and field-cooled data. The magnetic susceptibility increases on going from the LT-$LiCoO_2$ to the spinel $Li_{1-x}Co_2O_{4-\delta}$ (Fig. 7a), which is in

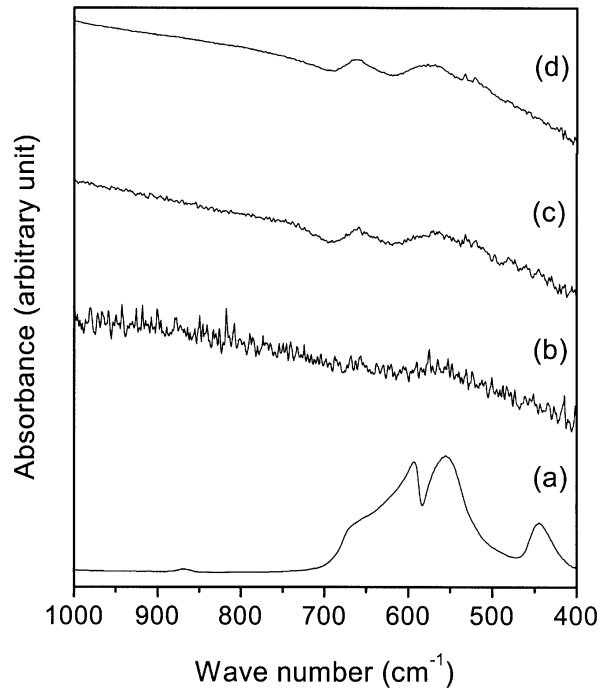

FIG. 6. Infrared spectra of (a) LT-$LiCoO_2$, (b) $LiCo_2O_{4-\delta}$, (c) $Li_{0.6}Co_2O_{4-\delta}$, and (d) $Li_{0.44}Co_2O_{4-\delta}$.

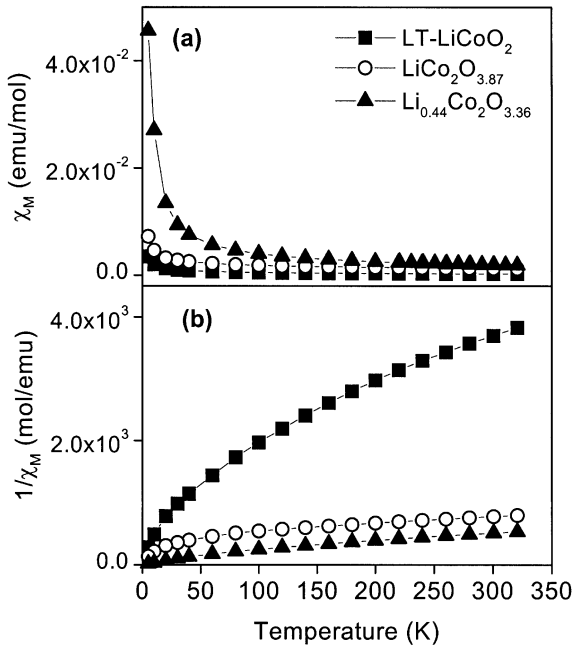

FIG. 7. Variations of (a) molar magnetic susceptibility and (b) inverse molar magnetic susceptibility with temperature for LT-$LiCoO_2$ and $Li_{1-x}Co_2O_{4-\delta}$ spinel oxides. The data shown were collected under the field-cooled condition with 5000 Oe.

accordance with the oxidation of low-spin Co^{3+} ions and introduction of holes into the Co:t_{2g} band on extracting lithium from the LT-$LiCoO_2$. Additionally, the magnetic susceptibility becomes nearly temperature independent with a large negative Weiss constant for the $Li_{1-x}Co_2O_{4-\delta}$ spinel samples (Fig. 7b) indicating a Pauli paramagnetic behavior with itinerant electrons.

4. CONCLUSIONS

$Li_{1-x}Co_2O_{4-\delta}$ samples crystallizing in the normal cubic spinel structure have been synthesized successfully for $0.44 \leq (1-x) \leq 1$ by an ambient temperature soft chemistry procedure. An overlap of the $Co^{3+/4+}$:3*d* band with the top of the O:2*p* band leads to the formation of a significant amount of oxygen vacancies during the extraction of lithium from the LT-$LiCoO_2$. The $Li_{1-x}Co_2O_{4-\delta}$ spinel oxides exhibit metallic behavior due to direct Co–Co interaction through the partially filled t_{2g} band although the samples with $(1-x)<1$ tend to show some localization due to the increasing amount of oxygen vacancies. In this regard, the electronic properties of the spinel $Li_{1-x}Co_2O_{4-\delta}$ oxides having 90° Co–O–Co and direct Co–Co interactions are similar to that of the perovskite $La_{1-x}Sr_xCoO_{3-\delta}$ oxides having 180° Co–O–Co interactions (29–31). However, the latter system becomes ferromagnetic with increasing $Co^{3+/4+}$ concentration while the former system does not due to the differences in the type of interactions. The study demonstrates that metastable phases having unusually high oxidation states and exhibiting interesting physical properties can be accessed at ambient temperatures by novel soft chemistry routes.

ACKNOWLEDGMENTS

This work was supported by the Welch Foundation Grant F-1254, Center for Space Power at the Texas A&M University (a NASA Commercial Space Center), and Texas Advanced Technology Program Grant 003658-0488-1999.

REFERENCES

1. J. Zaanen, G. A. Zawatzky, and J. W. Allen, *Phys. Rev. Lett.* **55,** 418 (1985).
2. J. G. Bednorz and K. A. Muller, *Z. Phys. B* **64,** 189 (1986).
3. R. Von Helmolt, J. Wecker, B. Holzapfelh, L. Schultz, and K. Samwer, *Phys. Rev. Lett.* **71,** 2331 (1993).
4. J. B. Torrance, P. Lacorre, C. Asavaroengchai, and R. M. Metzger, *J. Solid State Chem.* **90,** 168 (1991).
5. J. B. Torrance, P. Lacorre, C. Asavaroengchai, and R. M. Metzger, *Physica C* **182,** 351 (1991).
6. J. B. Torrance, P. Lacorre, A. I. Nazzal, E. J. Ansaldo, and Ch. Niedermayer, *Phys. Rev. B* **45,** 8209 (1992).
7. K. Mizushima, P. C. Jones, P. J. Wisemand, and J. B. Goodenough, *Mater. Res. Bull.* **15,** 783 (1980).
8. J. B. Goodenough, K. Mizushima, and T. Takeda, *Jpn. J. Appl. Phys.* **19,** 305 (1980).
9. T. Ohzuku, A. Ueda, and M. Nagayama, *J. Electrochem. Soc.* **140,** 1862 (1993).
10. G. G. Amatucci, J. M. Tarascon, and L. C. Klein, *J. Electrochem. Soc.* **143,** 1114 (1996).
11. J. M. Tarascon, G. Vaughan, Y. Chabre, L. Seguin, M. Anne, P. Strobel, and G. Amatucci, *J. Solid State Chem.* **147,** 410 (1999).
12. L. Croguennec, C. Pouillerie, and C. Delmas, *J. Electrochem. Soc.* **147,** 1314 (2000).
13. R. V. Chebiam, F. Prado, and A. Manthiram, *Chem. Mater.* **13,** 2951 (2001).
14. A. Manthiram, R. V. Chebiam, and F. Prado, *Mater. Res. Soc. Symp. Proc.* **658,** GG8-12-1 (2001).
15. R. J. Gummow, M. M. Thackeray, W. I. F. David, and S. Hull, *Mater Res. Bull.* **27,** 327 (1992).
16. R. J. Gummow, D. C. Liles, and M. M. Thackeray, *Mater Res. Bull.* **28,** 235 (1993).
17. R. J. Gummow, D. C. Liles, and M. M. Thackeray, *Mater Res. Bull.* **28,** 1177 (1993).
18. Y. Shao-Horn, S. A. Hackney, C. S. Johnson, A. J. Kahaian, and M. M. Thackeray, *J. Solid State Chem.* **140,** 116 (1998).
19. B. Garcia, P. Barboux, F. Ribot, A. Kahn-Harari, L. Mazerolles, and N. Baffier, *Solid State Ionics* **80,** 111 (1995).
20. B. Garcia, J. Farcy, J. P. Pereira-Ramos, J. Perichon, and N. Baffier, *J. Power Sources* **54,** 373 (1995).
21. B. Garcia, J. Farcy, and J. P. Pereira-Ramos, *J. Electrochem. Soc.* **144,** 1179 (1997).
22. R. A. Young, A. Shakthivel, T. S. Moss, and C. O. Paiva Santos, *J. Appl. Crystallogr.* **28,** 366 (1995).
23. A. Manthiram, J. S. Swinnea, Z. T. Sui, H. Steinfink, and J. B. Goodenough, *J. Am. Chem. Soc.* **109,** 6667 (1987).
24. M. M. Thackeray, W. I. F. David, P. G. Bruce, and J. B. Goodenough, *Mater. Res. Bull.* **18,** 461 (1983).
25. L. A. Montoro, M. Abbate, and J. M. Rosolen, *Electrochem. Solid State Lett.* **3,** 410 (2000).

26. A. Hightower, J. Graetz, C. C. Ahn, P. Rez, and B. Fultz, 198th Meeting of the Electrochemical Society, Phoenix, AZ, October 22–27, 2000, Abstract No. 177.
27. A. Manthiram and J. B. Goodenough, *Can. J. Phys.* **65,** 1309 (1987).
28. M. Menetrier, I. Saadoune, S. Levasseur, and C. Delmas, *J. Mater. Chem.* **9,** 1135 (1999).
29. R. Mahendiran and A. K. Raychaudhuri, *Phys. Rev. B* **54,** 16044 (1996).
30. M. A. Señarís-Rodríguez, and J. B. Goodenough, *J. Solid State Chem.* **118,** 323 (1995).
31. R. Caciuffo, D. Rinaldi, G. Barucca, J. Mira, J. Rivas, M. A. Señarís-Rodríguez, P. G. Radaelli, D. Fiorani, and J. B. Goodenough, *Phys. Rev. B* **59,** 1068 (1999).